

## The 3D Visualization of $E_8$ using an $H_4$ Folding Matrix

J Gregory Moxness\*  
*TheoryOfEverything.org*  
 (Dated: November 14, 2014)

This paper will present various techniques for visualizing a split real even  $E_8$  representation in 2 and 3 dimensions using an  $E_8$  to  $H_4$  folding matrix. This matrix is shown to be useful in providing direct relationships between  $E_8$  and the lower dimensional Dynkin and Coxeter-Dynkin geometries contained within it, geometries that are visualized in the form of real and virtual 3 dimensional objects. A direct linkage between  $E_8$ , the folding matrix, fundamental physics particles in an extended Standard model, quaternions, and octonions is introduced, and its importance is investigated and described.

PACS numbers: 02.20.-a, 61.44.Br, 04.50.-h, 04.60.Cf

Keywords: Coxeter groups,  $E_8$ , root systems, particle physics, string theory

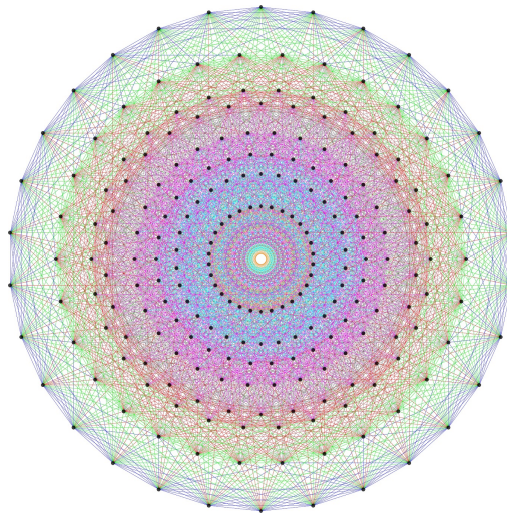


FIG. 1:  $E_8$  Petrie projection

### I. INTRODUCTION

Fig. 1 is the Petrie projection of the largest of the exceptional simple Lie algebras, groups and lattices called  $E_8$ . It has 240 vertices and 6720 edges of 8 dimensional (8D) length  $\sqrt{2}$ . Interestingly, in addition to containing the 8D structures of  $D_8$  and  $BC_8$  (aka. the 8 demicube or alternated octeract),  $E_8$  has been shown to fold to the 4D Polychora of  $H_4$  (aka. the 120 vertex 600-cell) and a scaled copy  $H_4/\varphi$ , where  $\varphi = \frac{1}{2}(1 + \sqrt{5})$  is the Golden Ratio[10][20]. Fig. 2 shows the folding orientation of  $E_8$  and D6 Dynkin diagrams above the  $H_4$  and  $H_3$  Coxeter-Dynkin diagrams (respectively).

The 600-cell is constructed from the combination of the 96 vertices of the snub 24-cell and the 24 vertices of the 24-cell shown in Fig. 3. The 24-cell is self-dual and contained within both  $F_4$  and the triality symmetry of the  $D_4$  Dynkin diagram. It is interesting to note that it is constructed from the 16 vertices of the  $BC_4$  tesseract (or 8-cell or 4-cube) and the 8 vertices of it's dual, the 4-orthoplex (or 16-cell). All of these polychora can be found within  $E_8$  with the excluded 8-orthoplex. The snub 24-cell is constructed from even permutations of  $\{\varphi, 1, 1/\varphi, 0\}$ . Also shown in Fig. 3 is the dual of the 600-cell, namely the 120-cell with 600 vertices and a trirectified  $H_4$  Coxeter-Dynkin diagram (i.e. the filled node is moved to the other end).

---

\*URL: <http://TheoryOfEverything.org/MyToE>; Electronic address: <mailto:JGMoxness@TheoryOfEverything.org>

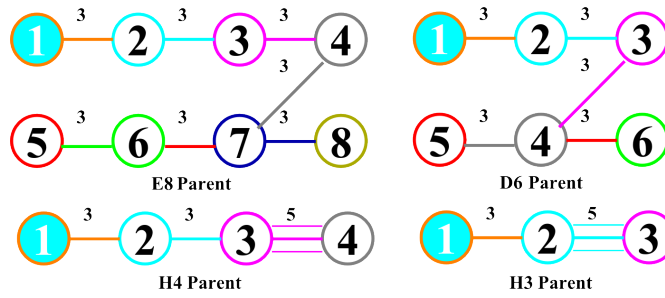


FIG. 2:  $E_8$  and  $D_6$  Dynkin diagrams in folding orientation with their associated Coxeter-Dynkin diagrams  $H_4$  and  $H_3$

### 4D Perspective Projections

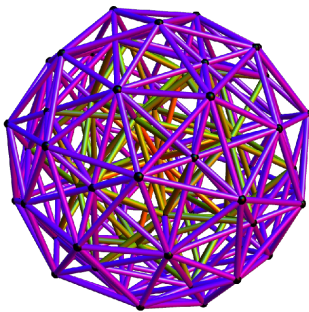
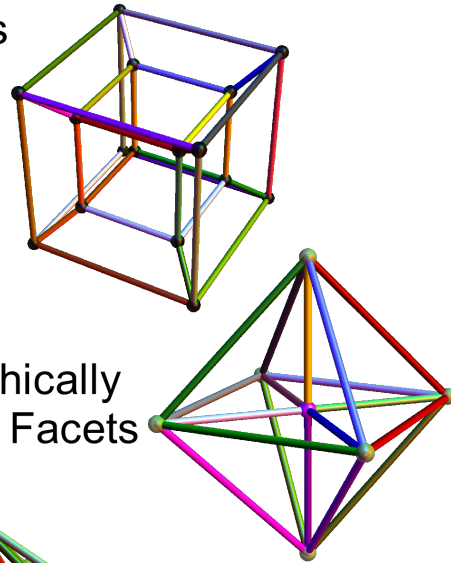
BC4 8-Cell=4-Cube=  
Tesseract;

Orthographically projects  
to a 3-Cube

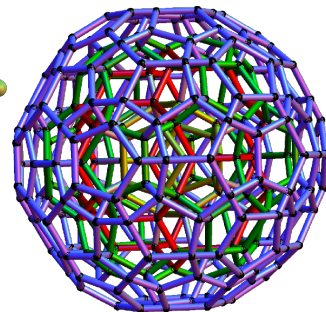
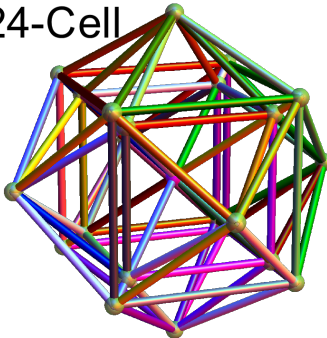
+ 16-Cell=4-Orthoplex=

Dual of 4-Cube; Orthographically  
projects to an Octahedron; Facets  
contain A3 3-Simplex

= D4 Self-Dual 24-Cell



H4 600-Cell=  
24-Cell+Snub 24-Cell



120-Cell=  
Dual of 600-Cell

FIG. 3: 4D Polychora

$$H_{4\text{fold}} = \begin{pmatrix} \varphi^2 & 0 & 0 & 0 & 1/\varphi & 0 & 0 & 0 \\ 0 & 1 & \varphi & 0 & 0 & -1 & \varphi & 0 \\ 0 & \varphi & 0 & 1 & 0 & \varphi & 0 & -1 \\ 0 & 0 & 1 & \varphi & 0 & 0 & -1 & \varphi \\ 1/\varphi & 0 & 0 & 0 & \varphi^2 & 0 & 0 & 0 \\ 0 & -1 & \varphi & 0 & 0 & 1 & \varphi & 0 \\ 0 & \varphi & 0 & -1 & 0 & \varphi & 0 & 1 \\ 0 & 0 & -1 & \varphi & 0 & 0 & 1 & \varphi \end{pmatrix} \quad (1)$$

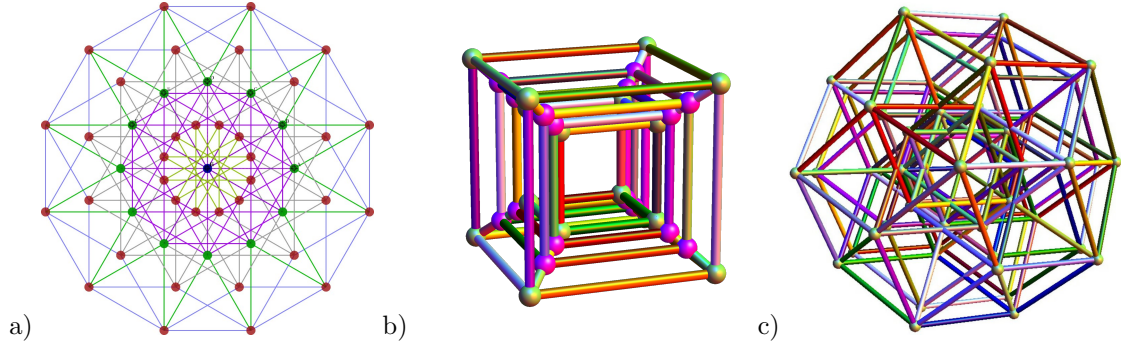


FIG. 4: The 6-cube a) Petrie projection b) 3D perspective c) rhombic triacontahedron

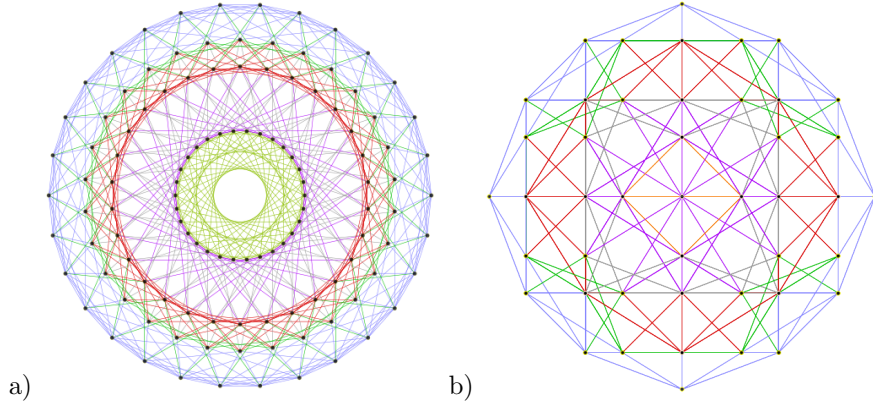


FIG. 5:  $H_4$  600-cell 2D projections: a) Van Oss (or Petrie), b) orthonormal

The specific matrix for performing this folding of  $E_8$  group vertices was shown[16] several years ago to be that of (1). Notice that  $H_{4\text{fold}} = H_{4\text{fold}}^T$  such that it is symmetric with a quaternion-octonion Cayley-Dickson like structure. Only the first 4 rows are needed for folding  $E_8$  to  $H_4$ , but the  $8 \times 8$  square matrix is useful in the rotation of 8D vectors by taking its inverse.

$E_8$  also contains the 6D structures of the 6-cube or hexeract as shown in Fig. 4. It has been shown that using rows 2 through 4 of  $H_{4\text{fold}}$  projects the 6-cube[1] down to the 3D Rhombic Triacontahedron[3]. This particular object is interesting in that it contains the Platonic solids including the icosahedron and dodecahedron, and has been used to describe the  $\varphi$  related geometry leading to quasicrystals[2].

$$\begin{aligned}
 x &= \{0 & (1 + \sqrt{5}) \sin \left[ \frac{\pi}{30} \right] & 0 & 1 & 0 & 0 & 0 & 0 \} \\
 y &= \{ (1 + \sqrt{5}) \sin \left[ \frac{\pi}{15} \right] & 0 & 2 \sin \left[ \frac{2\pi}{15} \right] & 0 & 0 & 0 & 0 & 0 \} \\
 z &= \{0 & 1 & 0 & (1 + \sqrt{5}) \sin \left[ \frac{\pi}{30} \right] & 0 & 0 & 0 & 0 \}
 \end{aligned} \tag{2}$$

$$\begin{aligned}
 X &= \{0 & 0.33821 & 1.2095 & 0.61803 & 0 & -0.33826 & -0.79094 & 0.61803\} \\
 Y &= \{1.08863 & 0.50275 & 0 & 0.81347 & -0.25699 & 0.50275 & 0 & -0.81347\} \\
 Z &= \{0 & 1 & 0.95629 & 0.20905 & 0 & -1 & 0.27977 & 0.20905\}
 \end{aligned} \tag{3}$$

Projection  $E_8$  to 2D (or 3D) requires 2 (or 3) basis vectors  $\{X, Y, Z\}$ . We start with (2), which are simply the two 2D Petrie projection basis vectors of the 600-cell (aka. the Van Oss projection) as shown in Fig. 5 a), with a 3rd  $z$  basis vector added for the 3D projection. Notice the 8D basis vectors with zero in the last 4 columns (or dimensions).

The  $E_8$  projection basis (3) is obtained by  $\{X, Y, Z\} = 4 * H_{4\text{fold}}^{-1} \cdot \{x, y, z\}$ . On one face (or 2 of 6 cubic faces, which are the same), they project  $E_8$  to its 2D Petrie projection shown in Fig. 1. On another face of this particular 3D projection is what would be found on all 6 faces of an orthonormal projection to 3D of the  $H_4$  600-cell combined with a scaled  $H_4/\varphi$ , shown in 2D on Fig. 5 b) and in 3D in Fig. 6.

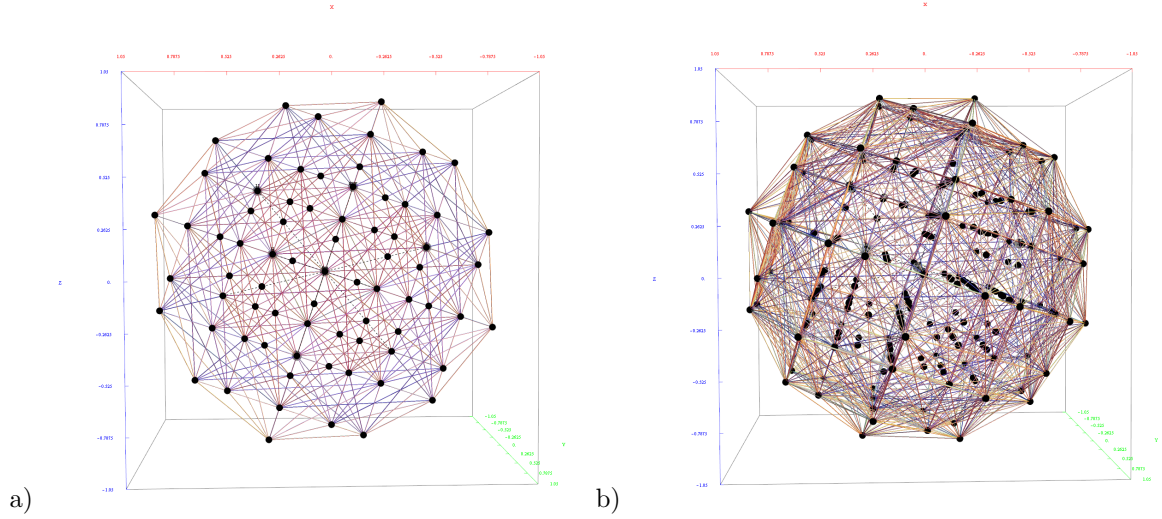


FIG. 6:  $E_8$  projection showing  $H_4$  and  $H_4/\varphi$  orthonormal face orientation in 2D and 3D perspective. Only 1220 of 6720 edges are shown in order prevent occlusion of vertices in 3D.

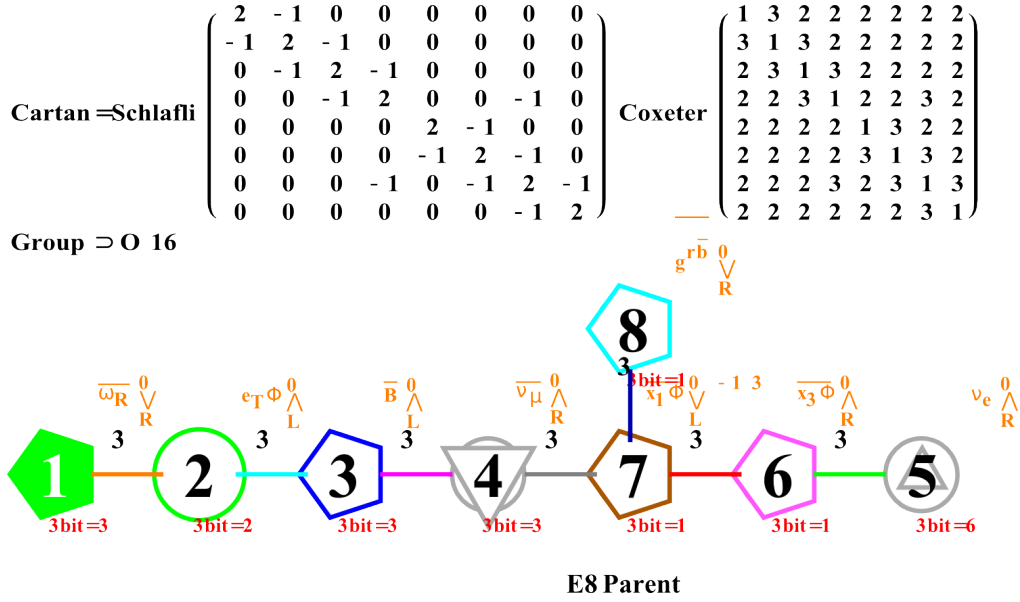


FIG. 7:  $E_8$  Dynkin diagram with Cartan, Schläfli, and Coxeter matrices

$$E8_{\text{srm}} = \begin{pmatrix} 1 & -1 & 0 & 0 & 0 & 0 & 0 & 0 \\ 0 & 1 & -1 & 0 & 0 & 0 & 0 & 0 \\ 0 & 0 & 1 & -1 & 0 & 0 & 0 & 0 \\ 0 & 0 & 0 & 1 & -1 & 0 & 0 & 0 \\ -\frac{1}{2} & -\frac{1}{2} \\ 0 & 0 & 0 & 0 & 0 & 1 & 1 & 0 \\ 0 & 0 & 0 & 0 & 1 & -1 & 0 & 0 \\ 0 & 0 & 0 & 0 & 0 & 1 & -1 & 0 \end{pmatrix} \quad (4)$$

There are several choices for the form of  $E_8$ , whether it be complex or split real (even or odd). For the purposes of this work, the form selected is split real even (SRE). While the basic topology of the  $E_8$  Dynkin diagram is unique, it has  $8! = 40320$  permutations of node ordering. The node order used here is given in Fig. 7. The 240 specific  $E_8$  group vertex values are determined from the simple roots matrix  $E8_{\text{srm}}$  shown in (4). The resulting Cartan matrix and generated algebraic roots are directly dependent on these as inputs.

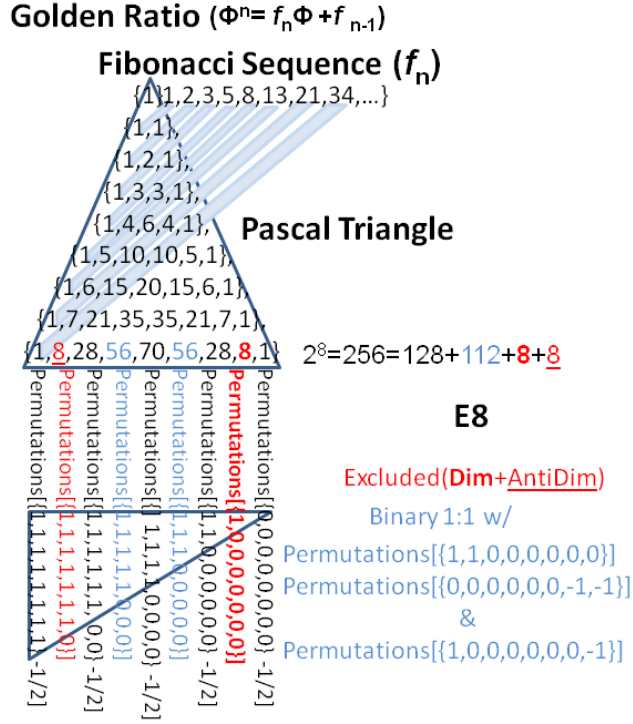


FIG. 8: SRE  $E_8$  construction from Pascal Triangle,  $Cl_8$  Clifford Algebra and binary permutations

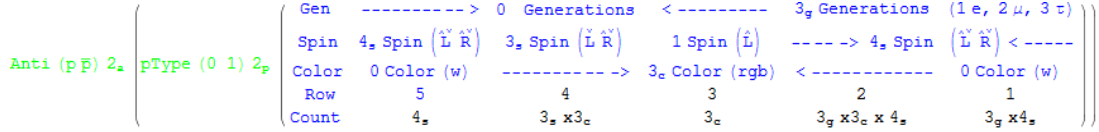


FIG. 9: Particle flavor counts given quantum number assignments

$$E8_{\text{Cartan}} = E8_{\text{srm}} \cdot E8_{\text{srm}}^T \quad (5)$$

$$E8_{\text{SREvertex}} = E8_{\text{srm}}^T \cdot E8_{\text{root}} \quad (6)$$

The Dynkin diagram was constructed as user input with the [Mathematica “VisibLie” notebook](#). Fig. 7 was generated and exported from the referenced tool, as are all of the figures in this paper. It has the same node ordering as the  $E_8$  Dynkin used in Fig. 2, but is now shown with the assigned physics particles with SRE  $E_8 \# \{206, 194, 184, 176, 1, 169, 170, 166\}$  that make up the simple roots matrix row entries of (4). The Cartan matrix can be generated directly by the structure of the Dynkin diagram or from its relationship to the simple roots matrix (5). The positive  $E_8$  algebra roots are generated by the Mathematica [“SuperLie” package](#) and listed in Fig. ?? along with its Hasse diagram in Fig. ?? of Appendix A. The 120 positive and 120 negative algebra roots are then used to generate the SRE  $E_8$  vertices using (6).

### $E_8$ GraviGUT Extended Standard Model Construction

Lisi has proposed an extended Standard Model (SM) GraviGUT based on an  $E_8$  Lie Algebra with a fundamental physics particle associated with each of its 240 roots[11]. While the particle assignments were modified from his original model to his current model[12], the model used here is closer to the

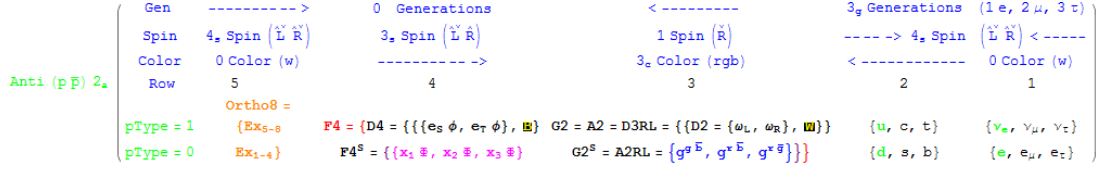


FIG. 10: Particle flavors in row / column groups with boson {group} coloring based on Lie group assignments ( $F_4$ ,  $F_4^s$ ,  $D_4$ & $G_2$ ,  $G_2^s$ )

original. It is modified slightly in order to create a complete 8-bit quantum pattern consistent with Figures 9 and 10. The complete  $E_8$  vertex to particle and octonion assignments are listed for reference in Figures ?? through ?? of Appendix B. The construction of this model is based on the 256 =  $2^8$  binary pattern from the 9th row of the Pascal triangle {1, 8, 28, 56, 70, 56, 28, 8, 1} and its associated  $Cl_8$  Clifford Algebra, shown in Fig. 8.

In this model, the 16 particles associated with columns 2 and 8 of the 9th row of the Pascal triangle {8, 8} are excluded as dimensional generators from the permutations of  $\{\pm 1, 0, 0, 0, 0, 0, 0\}$ . These excluded particles are associated with the 8-orthoplex (dual of the 8-cube with 256 vertices). While the positive generators are added to the “dimension count” of  $E_8$ , they are not included as vertices per se, but they do show up in the projections as the axis of the basis vectors. This leaves  $E_8$  with its 120 positive roots and 120 negative roots in the other 7 columns of the Pascal triangle.

The SRE  $E_8$  roots are defined by combining the 112 = {56, 56} integer roots of Lie group  $D_8$  = SO(16) with 128 = {1, 28, 70, 28, 1} half integer roots of Lie group  $BC_8$  = Sp(16). Specifically,  $D_8$  contains all permutations of  $\{\pm 1, \pm 1, 0, 0, 0, 0, 0, 0\}$  and  $BC_8$  contains all permutations of  $\{\pm 1, \pm 1\}/2$  with an even number of plus signs (an 8 demicube or even 7-cube).

There are 48 assigned  $D_8$  integer bosons and only 128  $C_8$  half-integer vertices available. Yet, with 192 =  $64 * 3$  generation fermions in SM, the meaning or validity of assigning a generation of fermions to the remaining 64  $D_8$  integer vertices has been hotly debated[7]. In this model, the remaining 64 integer vertices are assigned to the 2nd generation fermions. For a complete reference of particle assignments, see Appendix B.

The specific particle assignments are determined by the configuration of the particle {spin, color, generation, flavor and type} and the patterns within  $E_8$ . The particle type  $\{e, \nu_e\}$  or  $\{u, d\}$  and spin  $\{\overset{\vee}{L}, \overset{\wedge}{R}, \overset{\vee}{L}, \overset{\vee}{R}\}$  are assigned or encoded in the positions or dimensions {1, 2, 3, 4} of each  $E_8$  vertex. The generations are encoded in position {5}, and color in positions {6, 7, 8}. The antiparticle operation is simply the negation of the  $E_8$  vertex (or in the binary representation “inverted”  $0 \Leftrightarrow 1$  as shown in Fig. 8). It should be noted that although the positive roots of the algebra are not all assigned as “particles”, the negation of the root does represent the “anti” particle operation on the assigned particle. The charge calculation for the particles is obtained by  $Q = E_{8SREvertex} \cdot \{0, 0, 0, -3, 0, 1, 1, 1\}/3$ . This provides accurate results for the generation 0 bosons and 1st and 3rd generation fermions. It shows interesting deviations for some of the 2nd generation fermions that have been assigned to the  $D_8$  integer vertices.

It is also helpful to note that the entire binary and SRE vertex list (as constructed in Fig. 8 and listed in Appendix B) is lexicographically ordered from negative to positive with a left-right and bottom-top mirroring about the middle, between the 128th and 129th of 256 vertices, which are the  $\hat{R}$  tau neutrinos  $\nu_\tau$  and  $\bar{\nu}_\tau$ . Also of interest are the first and last vertex particles which are rows {1, 9} of the Pascal Triangle with all 0 or all 1/2 entries. These are the  $\hat{R}$  electron neutrinos  $\nu_e$  and  $\bar{\nu}_e$ . This integrated model aligns well with the idea that it is associated with (T)ime reversal in the Charge-Parity-Time (CPT) conservation laws and points to the special consideration needed for the right handed neutrinos in the SM.

## II. THE QUANTUM BIT-WISE PARTICLE ASSIGNMENTS

$$E_8 \text{ Dynkin}_3 \text{ bit} = \begin{pmatrix} \mathbf{3bit} = & 0 & 1 \\ 4 = 2^2 & \mathbf{g0} & \text{Boson Fermion} \\ & & \text{Gen 0-2 Gen 1-3} \\ 2 = 2^1 & \mathbf{p} & e/d \quad \nu/u \\ 1 = 2^0 & \mathbf{a} & p \quad \bar{p} \end{pmatrix} \quad (7)$$

The 1:1 bit-wise correspondence of a particle's quantum number assignments is a big-endian (left most significant) zero-based 8 dimensional vector  $\{7-0\}$ . The assignments are {1 antiparticle bit= $\{\mathbf{a}\}(p/\bar{p})$ , 1  $p_{\text{type}}$  bit= $\{\mathbf{p}\}(e/\nu$  leptons or u/d quark), 2 color bits= $\{c1, c0\}$ (w=0 or none/r/g/b), 2 spin bits= $\{s1, s0\}(\check{L}, \hat{R}, \hat{L}, \check{R})$ , and 2 generation bits= $\{g1, \mathbf{g0}\}$ (0=bosons/ $e/\mu/\tau$ )} or simply  $\{\mathbf{a}, \mathbf{p}, s1, s0, c1, c0, g1, \mathbf{g0}\}$ . The **bold** type face indicates quantum assignments which are not only allocated to an SRE  $E_8$  vertex dimension as described above, but are exhibited in the inherent structural symmetry of the  $E_8$  algebra, group or lattice. These **bold** bits are used to define the 3 bit structure of (7) associated with the  $E_8$  Dynkin diagram in Fig. 7.

$$\text{Physics}_{\text{rot}} = \begin{pmatrix} 1 & 0 & 0 & 0 & 0 & 0 & 0 & 0 \\ 0 & 1 & 0 & 0 & 0 & 0 & 0 & 0 \\ 0 & 0 & \frac{1}{\sqrt{2}} & -\frac{1}{\sqrt{2}} & 0 & 0 & 0 & 0 \\ 0 & 0 & \frac{1}{\sqrt{2}} & \frac{1}{\sqrt{2}} & 0 & 0 & 0 & 0 \\ 0 & 0 & 0 & 0 & 1 & 0 & 0 & 0 \\ 0 & 0 & 0 & 0 & 0 & \frac{1}{\sqrt{3}} & \frac{1}{\sqrt{3}} & \frac{1}{\sqrt{3}} \\ 0 & 0 & 0 & 0 & 0 & -\frac{1}{\sqrt{2}} & \frac{1}{\sqrt{2}} & 0 \\ 0 & 0 & 0 & 0 & 0 & -\frac{1}{\sqrt{6}} & -\frac{1}{\sqrt{6}} & \sqrt{\frac{2}{3}} \end{pmatrix} \quad (8)$$

$$\text{Fermionic Triality}_{\text{rot}} = \frac{1}{2} \begin{pmatrix} -1 & 1 & 1 & -1 & 0 & 0 & 0 & 0 \\ -1 & 1 & -1 & 1 & 0 & 0 & 0 & 0 \\ -1 & -1 & 1 & 1 & 0 & 0 & 0 & 0 \\ 1 & 1 & 1 & 1 & 0 & 0 & 0 & 0 \\ 0 & 0 & 0 & 0 & -1 & -1 & -1 & -1 \\ 0 & 0 & 0 & 0 & 1 & 1 & -1 & -1 \\ 0 & 0 & 0 & 0 & 1 & -1 & 1 & -1 \\ 0 & 0 & 0 & 0 & 1 & -1 & -1 & 1 \end{pmatrix} \quad (9)$$

$$\text{Bosonic Triality}_{\text{rot}} = \frac{1}{3} \begin{pmatrix} 3 & 0 & 0 & 0 & 0 & 0 & 0 & 0 \\ 0 & 0 & 0 & -3 & 0 & 0 & 0 & 0 \\ 0 & 3 & 0 & 0 & 0 & 0 & 0 & 0 \\ 0 & 0 & -3 & 0 & 0 & 0 & 0 & 0 \\ 0 & 0 & 0 & 0 & 0 & 0 & 0 & 0 \\ 0 & 0 & 0 & 0 & 0 & -2 & -1 & 2 \\ 0 & 0 & 0 & 0 & 0 & 2 & -1 & -1 \\ 0 & 0 & 0 & 0 & 0 & -1 & 2 & -1 \end{pmatrix} \quad (10)$$

As already described for the  $E_8$  vertices, the  $\{\mathbf{a}\}$  bit splits the 128 particles from 128 anti-particles. The  $\{\mathbf{g0}\}$  bit splits the generation 0 boson family of 128(=112 integer roots of  $D_8+16$  excluded integer roots of the 8-orthoplex) from the 128 half integer root (and half integer spin) of  $C_8$  fermions. The  $\{\mathbf{p}\}$  bit splits all particle families into two types, referenced in the leptons as electron and neutrino types, while the quarks are designated by up and down types. It splits the integer bosons into 2 types as well, which is a key feature of this model over the original Lisi model.

These differences are most easily seen in the  $8 \times 8$  rotation matrix used for transforming SRE coordinates to physics coordinates (8) and those matrices used in identifying fermionic (9) and bosonic (10) triality transformations. Just as the  $E_8$  to  $H_4$  folding matrix has symmetric quaternion quadrants in the octonion matrix, the physics and triality rotation matrices are divided by an upper left quadrant affecting the SRE {1-4} spin positions and a lower right quadrant affecting the SRE {5-8} generation-color positions. As a matter of fact, the physics rotation clearly operates on the SRE  $E_8$  vertices by pairing them into 4 sets, specifically  $p_{\text{type}}$  {1,2}, spin {3,4}, generation {5,6} and color {7,8}. This physics rotation is more dramatically shown in the next section on triality.

Visualizing this  $E_8$  based physics model by projection to 2D and 3D with vertex shape, size and color assigned based on the described patterns is now possible. Using the direct relationship to lower dimensional geometry symmetries provided by the folding matrix provides the flexibility to select the contents of the visualization based on the quantum physics parameters of the model and not just the math of the geometry. A few examples are shown in Fig. 11.

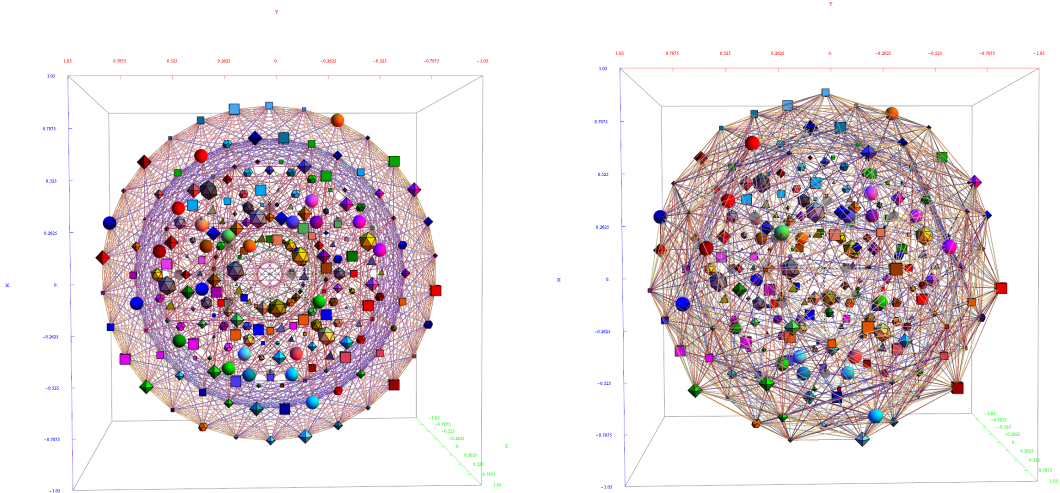


FIG. 11:  $E_8$  showing the Petrie projection face orientation in 2D and 3D perspective with vertices as physics particle assignments. Vertex shape, size, color/shade are assigned based on extended Standard Model particle assignments. Only 1220 of 6720 edges are shown in order prevent occlusion of vertices in 3D perspective.

### Triality Relationships

The Lisi model also demonstrates a consistency with the bosons and fermions that is related to the triality relationships within  $E_8$ . This is shown in Fig. 12 with blue triality lines linking the 3 generations of each fermion using (9). Applying the triality rotation matrix as a dot product against an SRE vector gives the 2nd generation fermion particle. Applying it again gives the 3rd generation. Applying it a 3rd time returns to the 1st generation fermion. The bosons are also involved in triality relationships as well using (10), rotating through red, green, and blue particle color assignments.

It is interesting to note that the quarks  $\{r/g/b, p/\bar{p}\}$  are all located on 6 corresponding dual concentric circles around the center. The leptons are hexagonal “Star of David“ patterns in the center, while the bosons are in single or dual hexagonal rings radiating from the center.

$$\text{Triality}_{\text{basis}} \begin{aligned} H &= \left\{ 2 - \frac{4}{\sqrt{3}}, 0, 0, \sqrt{2} - \sqrt{\frac{2}{3}}, 0, 0, \sqrt{2}, 0 \right\} \\ V &= \left\{ 0, \frac{4}{\sqrt{3}} - 2, \sqrt{\frac{2}{3}} - \sqrt{2}, 0, 0, 0, 0, -\sqrt{2} \right\} \end{aligned} \quad (11)$$

The axis shown in Fig. 12 are rotated to physics coordinates using (8), which puts the basis vectors (11) on the projected (H)orizontal and (V)ertical axis. It seems to clarify dimensional identities as well. For example, when the  $\{1, 2, 3\}$  dimensions are moved (i.e. using axis locators in the tool), all vertices change positions except the  $p_{\text{type}=0}$  bosons  $\{g \text{ gluons}, x_n \Phi\}$ . Moving dimension  $\{4\}$  preserves these as well as the  $\hat{L}$  and  $\check{R}$  quark positions. Moving the dimensions  $\{5, 6\}$  preserves these, except now the row 4  $p_{\text{type}=0}$  bosons  $\{x_n \Phi\}$  emerge from the 6 triple overlap points at center of the quark’s concentric rings (the intersection of the gluons triality lines). And finally, the  $\{7, 8\}$  dimensions in physics can be identified with quark color, as  $\{7\}$  preserves the blue quark positions, while  $\{8\}$  moves the dual concentric rings of quarks while preserving their relative positions within the rings. It is interesting to note that the dimensions  $\{6, 7, 8\}$  are appropriately labeled  $\{r, g, b\}$  in SRE coordinates, since in this projection the SRE math coordinates are located at the aforementioned 6 triple overlap points at center of the quark’s  $\{\bar{r}, g, \bar{g}, b, \bar{b}\}$  concentric rings (the intersection of the gluons triality lines).

### III. $E_8$ TO $H_4$ FOLDING’S APPLICATION TO THEORETICAL PHYSICS

$H_{4\text{fold}}$  provides a new and more direct relationship between  $E_8$  and its lower dimensional geometric objects such as  $H_4$ . This has allowed for improvements to  $E_8$  related physics models, such as those of Lisi[11]. This theoretical model is shown to provide  $E_{8\text{Srm}}$  assigned particles as fundamental building blocks for generating the rest of the 240  $E_8$  vertex mapped particles[14].



#### IV. OCTONIONS AND $E_8$ WITH $H_4$ FOLDING

In addition to mapping extended SM particle quantum bits between  $H_4$  and the SRE  $E_8$  vertices and algebra roots, they [have been mapped](#)[17] to the 480 unique permutations of octonions[5] and [the 3840 split octonions](#)[18] through a common pattern associated with the quantum bits. This octonionic mapping provides valuable insight into related theoretical physics models.

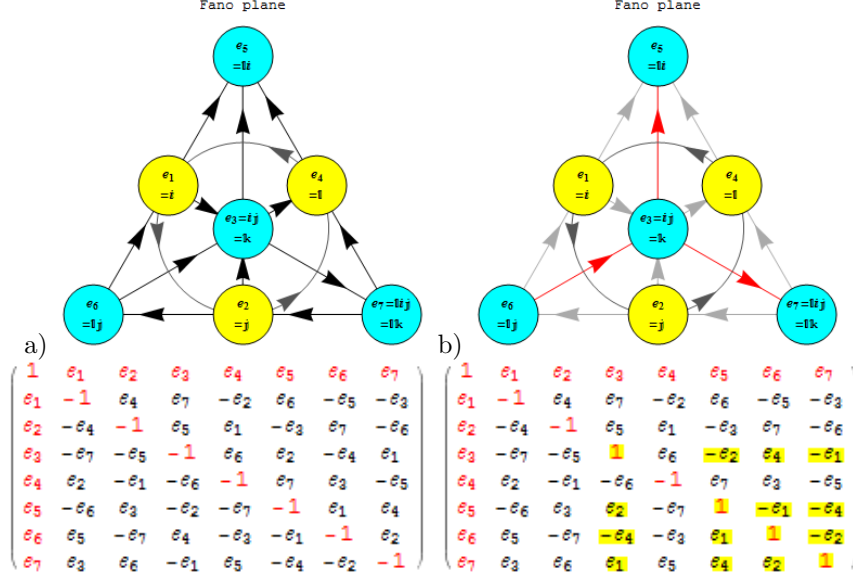


FIG. 13: Octonion representations: a) Fano plane, b) 1st triad split Fano plane

$$\text{Fano plane triads} \\ \{\{1, 2, 4\}, \{1, 3, 7\}, \{1, 5, 6\}, \{2, 3, 5\}, \{2, 6, 7\}, \{3, 4, 6\}, \{4, 5, 7\}\}$$

$$\text{Flattened triads} \\ \{1, \mathbf{4}, \mathbf{2}, 3, 7, 5, 6\} \quad (12)$$

$$\text{Mask bits} \\ \{0, 0, 0, 0, 0, 0, 0\}$$

The double cover of the 240 vertices requires the addition of a 9th “flip“ bit that operates on the Fano plane representation by reversing two of the midpoint nodes in the Fano plane triads (i.e. those with circular directed edges in Fig. 13). These node numbers are always indicated by the 2nd and 3rd columns of the flattened triads as shown in (12). They are bolded when reversed (or “flipped“), which shows this particular octonion has the flip bit set. The flattened triad is simply created by taking in sequence the numbers from the first triad along with the last two numbers in the 2nd and 3rd triads. It operates to define the node numbers for each canonical position of the Fano plane mnemonic.

As it was for the permutation of node numbers in Dynkin diagrams, there are many permutations of node number and arrow direction in the octonion Fano plane which are equivalent. What is important is the representation of the triads given in (12). This particular set of triads is equivalent to that used in Baez’ work on octonions[4].

$$\begin{aligned}
& \begin{array}{l}
1 \quad \{\{1, 2, 3\}, \{1, 4, 5\}, \{1, 6, 7\}, \{2, 4, 6\}, \{2, 5, 7\}, \{3, 4, 7\}, \{3, 5, 6\}\} \\
2 \quad \{\{1, 2, 3\}, \{1, 4, 5\}, \{1, 6, 7\}, \{2, 4, 7\}, \{2, 5, 6\}, \{3, 4, 6\}, \{3, 5, 7\}\} \\
3 \quad \{\{1, 2, 3\}, \{1, 4, 6\}, \{1, 5, 7\}, \{2, 4, 5\}, \{2, 6, 7\}, \{3, 4, 7\}, \{3, 5, 6\}\} \\
4 \quad \{\{1, 2, 3\}, \{1, 4, 6\}, \{1, 5, 7\}, \{2, 4, 7\}, \{2, 5, 6\}, \{3, 4, 5\}, \{3, 6, 7\}\} \\
5 \quad \{\{1, 2, 3\}, \{1, 4, 7\}, \{1, 5, 6\}, \{2, 4, 5\}, \{2, 6, 7\}, \{3, 4, 6\}, \{3, 5, 7\}\} \\
6 \quad \{\{1, 2, 3\}, \{1, 4, 7\}, \{1, 5, 6\}, \{2, 4, 6\}, \{2, 5, 7\}, \{3, 4, 5\}, \{3, 6, 7\}\} \\
7 \quad \{\{1, 2, 4\}, \{1, 3, 5\}, \{1, 6, 7\}, \{2, 3, 6\}, \{2, 5, 7\}, \{3, 4, 7\}, \{4, 5, 6\}\} \\
8 \quad \{\{1, 2, 4\}, \{1, 3, 5\}, \{1, 6, 7\}, \{2, 3, 7\}, \{2, 5, 6\}, \{3, 4, 6\}, \{4, 5, 7\}\} \\
9 \quad \{\{1, 2, 4\}, \{1, 3, 6\}, \{1, 5, 7\}, \{2, 3, 5\}, \{2, 6, 7\}, \{3, 4, 7\}, \{4, 5, 6\}\} \\
10 \quad \{\{1, 2, 4\}, \{1, 3, 6\}, \{1, 5, 7\}, \{2, 3, 7\}, \{2, 5, 6\}, \{3, 4, 5\}, \{4, 6, 7\}\} \\
11 \quad \{\{1, 2, 4\}, \{1, 3, 7\}, \{1, 5, 6\}, \{2, 3, 5\}, \{2, 6, 7\}, \{3, 4, 6\}, \{4, 5, 7\}\} \\
12 \quad \{\{1, 2, 4\}, \{1, 3, 7\}, \{1, 5, 6\}, \{2, 3, 6\}, \{2, 5, 7\}, \{3, 4, 5\}, \{4, 6, 7\}\} \\
13 \quad \{\{1, 2, 5\}, \{1, 3, 4\}, \{1, 6, 7\}, \{2, 3, 6\}, \{2, 4, 7\}, \{3, 5, 7\}, \{4, 5, 6\}\} \\
14 \quad \{\{1, 2, 5\}, \{1, 3, 4\}, \{1, 6, 7\}, \{2, 3, 7\}, \{2, 4, 6\}, \{3, 5, 6\}, \{4, 5, 7\}\} \\
15 \quad \{\{1, 2, 5\}, \{1, 3, 6\}, \{1, 4, 7\}, \{2, 3, 4\}, \{2, 6, 7\}, \{3, 5, 7\}, \{4, 5, 6\}\} \\
16 \quad \{\{1, 2, 5\}, \{1, 3, 6\}, \{1, 4, 7\}, \{2, 3, 7\}, \{2, 4, 6\}, \{3, 4, 5\}, \{5, 6, 7\}\} \\
17 \quad \{\{1, 2, 5\}, \{1, 3, 7\}, \{1, 4, 6\}, \{2, 3, 4\}, \{2, 6, 7\}, \{3, 5, 6\}, \{4, 5, 7\}\} \\
18 \quad \{\{1, 2, 5\}, \{1, 3, 7\}, \{1, 4, 6\}, \{2, 3, 6\}, \{2, 4, 7\}, \{3, 4, 5\}, \{5, 6, 7\}\} \\
19 \quad \{\{1, 2, 6\}, \{1, 3, 4\}, \{1, 5, 7\}, \{2, 3, 5\}, \{2, 4, 7\}, \{3, 6, 7\}, \{4, 5, 6\}\} \\
20 \quad \{\{1, 2, 6\}, \{1, 3, 4\}, \{1, 5, 7\}, \{2, 3, 7\}, \{2, 4, 5\}, \{3, 5, 6\}, \{4, 6, 7\}\} \\
21 \quad \{\{1, 2, 6\}, \{1, 3, 5\}, \{1, 4, 7\}, \{2, 3, 4\}, \{2, 5, 7\}, \{3, 6, 7\}, \{4, 5, 6\}\} \\
22 \quad \{\{1, 2, 6\}, \{1, 3, 5\}, \{1, 4, 7\}, \{2, 3, 7\}, \{2, 4, 5\}, \{3, 4, 6\}, \{5, 6, 7\}\} \\
23 \quad \{\{1, 2, 6\}, \{1, 3, 7\}, \{1, 4, 5\}, \{2, 3, 4\}, \{2, 5, 7\}, \{3, 5, 6\}, \{4, 6, 7\}\} \\
24 \quad \{\{1, 2, 6\}, \{1, 3, 7\}, \{1, 4, 5\}, \{2, 3, 5\}, \{2, 4, 7\}, \{3, 4, 6\}, \{5, 6, 7\}\} \\
25 \quad \{\{1, 2, 7\}, \{1, 3, 4\}, \{1, 5, 6\}, \{2, 3, 5\}, \{2, 4, 6\}, \{3, 6, 7\}, \{4, 5, 7\}\} \\
26 \quad \{\{1, 2, 7\}, \{1, 3, 4\}, \{1, 5, 6\}, \{2, 3, 6\}, \{2, 4, 5\}, \{3, 5, 7\}, \{4, 6, 7\}\} \\
27 \quad \{\{1, 2, 7\}, \{1, 3, 5\}, \{1, 4, 6\}, \{2, 3, 4\}, \{2, 5, 6\}, \{3, 6, 7\}, \{4, 5, 7\}\} \\
28 \quad \{\{1, 2, 7\}, \{1, 3, 5\}, \{1, 4, 6\}, \{2, 3, 6\}, \{2, 4, 5\}, \{3, 4, 7\}, \{5, 6, 7\}\} \\
29 \quad \{\{1, 2, 7\}, \{1, 3, 6\}, \{1, 4, 5\}, \{2, 3, 4\}, \{2, 5, 6\}, \{3, 5, 7\}, \{4, 6, 7\}\} \\
30 \quad \{\{1, 2, 7\}, \{1, 3, 6\}, \{1, 4, 5\}, \{2, 3, 5\}, \{2, 4, 6\}, \{3, 4, 7\}, \{5, 6, 7\}\}
\end{array}
\end{aligned} \tag{13}$$

$$\begin{aligned}
& \begin{array}{l}
1 \quad \{00, 07, 19, 1E, 2A, 2D, 33, 34\} \\
2 \quad \{01, 06, 18, 1F, 2B, 2C, 32, 35\} \\
3 \quad \{02, 05, 1B, 1C, 28, 2F, 31, 36\} \\
4 \quad \{03, 04, 1A, 1D, 29, 2E, 30, 37\} \\
5 \quad \{08, 0F, 11, 16, 22, 25, 3B, 3C\} \\
6 \quad \{09, 0E, 10, 17, 23, 24, 3A, 3D\} \\
7 \quad \{0A, 0D, 13, 14, 20, 27, 39, 3E\} \\
8 \quad \{0B, 0C, 12, 15, 21, 26, 38, 3F\}
\end{array}
\end{aligned} \tag{14}$$

$$\text{sm2fpi} = \{5, 8, 4, 3, 7, 6, 3, 2, 6, 5, 1, 4, 6, 7, 3, 3, 8, 6, 3, 1, 6, 6, 2, 3, 5, 8, 4, 4, 3, 7, 6\} \tag{15}$$

There are 30 canonical sets of 7 triads indexed with a Fano plane index (fpi) in (13). As in  $E_8$  with 16 of the  $2^8 = 256$  binary representations excluded from the group, there are 32 excluded octonions from the  $2^9 = 512$ . As in  $E_8$ , excluded particles are associated with the color=0, generation=0 (bosons) which are the positive (and negative) generators commonly associated with the 8-orthoplex with 16 permutations of  $\{\pm 1, 0, 0, 0, 0, 0, 0\}$ .

In order to make a valid octonion, each fpi gets one of 8 possible 7-bit sign masks (sm) applied (14). Since each sm can be “inverted” ( $0 \Leftrightarrow 1$  as we do with the anti-particle quantum bit), this gives  $16 * 30 = 480$  octonion permutations.

The sign mask operates on the triads by reversing the 2nd and 3rd numbers from canonical (numerical) order when the mask bit is set on that triad’s position. Each sign mask operation acting on the 30 fpi’s can be permuted in consistent ways to produce the many isomorphic sets of 480 octonions. Since they are bit-wise operations, the sign masks use hexadecimal notation with the first bit always 0. It is interesting to note that there are only 2 octonions that use a sign mask of 00H. The one shown and another discovered by Dixon[8].



## Bibliography

- [1] 6-cube. [en.wikipedia.org/wiki/6-cube](http://en.wikipedia.org/wiki/6-cube), 2011.
- [2] Quasicrystal. [en.wikipedia.org/wiki/Quasicrystal](http://en.wikipedia.org/wiki/Quasicrystal), 2011.
- [3] Rhombic Triacontahedron. [en.wikipedia.org/wiki/RhombicTriacontahedron](http://en.wikipedia.org/wiki/RhombicTriacontahedron), 2011.
- [4] J. C. Baez. The Octonions. *ArXiv e-prints math/010515*, May 2001.
- [5] D. Chesley. Twisted octonions. *Personal Website*, 1988.
- [6] CMS Collaboration. Observation of the diphoton decay of the Higgs boson and measurement of its properties. *ArXiv e-prints hep-ex/1407.0558*, July 2014.
- [7] J. Distler and S. Garibaldi. There is No “Theory of Everything” Inside  $E_8$ . *Communications in Mathematical Physics*, 298:419–436, September 2010.
- [8] G. Dixon. Octonion X-product orbits. *ArXiv e-prints hep-th/9410202*, October 1994.
- [9] A. Douglas and J. Repka. The GraviGUT Algebra Is not a Subalgebra of  $E_8$ , but  $E_8$  Does Contain an Extended GraviGUT Algebra. *SIGMA math.RT/1305.6946*, 10:72, July 2014.
- [10] M. Koca and N. Koca. Quaternionic Roots of  $E_8$  Related Coxeter Graphs and Quasicrystals. *Turkish Journal of Physics*, 22:421–436, May 1998.
- [11] A. G. Lisi. An Exceptionally Simple Theory of Everything. *ArXiv e-prints hep-th/0711.0770*, November 2007.
- [12] A. G. Lisi. An Explicit Embedding of Gravity and the Standard Model in  $E_8$ . *ArXiv e-prints gr-qc/1006.4908*, June 2010.
- [13] J. G. Moxness. A More Natural Reference Model Integrating Relativity and Quantum Mechanics. [www.vixra.org/abs/1006.0063](http://www.vixra.org/abs/1006.0063), 1998.
- [14] J. G. Moxness. Particle Count Reduction in an  $E_8$  Standard Model. [www.vixra.org/abs/1109.0005](http://www.vixra.org/abs/1109.0005), 2011.
- [15] J. G. Moxness. Simplified ToE Summary (w/124.443 GeV Higgs Mass Prediction). [theoryofeverything.org/TOE/JGM/ToEsummary.pdf](http://theoryofeverything.org/TOE/JGM/ToEsummary.pdf), 2012.
- [16] J. G. Moxness.  $E_8$  folding to  $H_4+H_4/\varphi$ . [www.theoryofeverything.org/pageid=1454](http://www.theoryofeverything.org/pageid=1454), 2013.
- [17] J. G. Moxness. The 480 octonions, their Fano planes and multiplication tables. [theoryofeverything.org/TOE/JGM/Fano.pdf](http://theoryofeverything.org/TOE/JGM/Fano.pdf), 2013.
- [18] J. G. Moxness. The Comprehensive Split Octonions and their Fano Planes. [theoryofeverything.org/TOE/JGM/splitFano.pdf](http://theoryofeverything.org/TOE/JGM/splitFano.pdf), 2013.
- [19] J. G. Moxness. In Work. [www.theoryofeverything.org/pageid=2189](http://www.theoryofeverything.org/pageid=2189), 2014.
- [20] David A. Richter. Triacontagonal coordinates for the  $E(8)$  root system. *ArXiv e-prints math.GM/0704.3091*, April 2007.

## VI. APPENDIX A

The positive  $E_8$  algebra roots generated by the Mathematica “SuperLie” package and its Hasse diagram. The full source version of the “VisibLie” notebook at <http://theoryofeverything.org/MyToE> may be made available by request in order to generate algebra roots and their Hasse diagrams.

See [E8toH4fold.pdf](#) for a full version with this appendix.

## VII. APPENDIX B

The comprehensive SRE  $E_8$  vertex, bitwise particle and octonion assignments. They are grouped by the Pascal Triangle / Clifford Algebra sort.

See [E8toH4fold.pdf](#) for a full version with this appendix.